

## CHEMISTRY

# Templated deprotonative metalation of polyaryl systems: Facile access to simple, previously inaccessible multi-iodoarenes

Antonio J. Martínez-Martínez,<sup>1\*</sup> Stephen Justice,<sup>1</sup> Ben J. Fleming,<sup>1</sup> Alan R. Kennedy,<sup>1</sup> Iain D. H. Oswald,<sup>2</sup> Charles T. O'Hara<sup>1†</sup>

The development of new methodologies to affect non-*ortho*-functionalization of arenes has emerged as a globally important arena for research, which is key to both fundamental studies and applied technologies. A range of simple arene feedstocks (namely, biphenyl, *meta*-terphenyl, *para*-terphenyl, 1,3,5-triphenylbenzene, and biphenylene) is transformed to hitherto unobtainable multi-iodoarenes via an *s*-block metal sodium magnesiate templated deprotonative approach. These iodoarenes have the potential to be used in a whole host of high-impact transformations, as precursors to key materials in the pharmaceutical, molecular electronic, and nanomaterials industries. To prove the concept, we transformed biphenyl to 3,5-bis(*N*-carbazolyl)-1,1'-biphenyl, a novel isomer of 4,4'-bis(*N*-carbazolyl)-1,1'-biphenyl (CPB), a compound which is currently widely used as a host material for organic light-emitting diodes.

## INTRODUCTION

Until 1938, organometallic reagents were considered as exotic rarities, commanding little application in synthetic chemistry (1). However, the discoveries by Gilman and Bebb (2) and Wittig *et al.* (3) that alkyllithium reagents could be used to selectively metalate anisole (and other heterosubstituted arenes) at an *ortho* position opened the doors to the first major utilization of organometallics in synthesis. This discovery was later coined *ortho*-metalation (DoM) (4), and from this juncture, organometallic reagents were seen as “indispensable tools in chemical synthesis” (1). DoM can be used to install new functionalities on arenes, thus allowing the construction of new molecules (5–7), and relies on converting a relatively inert C–H bond in an organic molecule into a more reactive and versatile C–metal bond by treating it with a metalating reagent (normally an organolithium reagent). The beauty of the DoM reaction is it efficiently and selectively metalates the C–H bond adjacent to a directing group (DG), which promotes reaction due to its dual coordination/inductive roles. Since the pioneering works of Gilman and Bebb (2) and Wittig *et al.* (3), the DoM concept has been advanced using monometallic (8–12) and bimetallic (13–19) systems.

In his influential text, Schlosser stated, “deviations from the *ortho*-rule do exist but are scarce” (1). Enabling activation of arene C–H bonds at positions other than *ortho* has become a high interest and impact area of research, with the goal of allowing easy access to key pharmaceuticals, agrochemicals, and novel materials. In the main, new methodologies involve transition metal C–H activation chemistry (20–28). In 2014, we exploited *s*-block organometallic chemistry and reported directed *ortho*-*meta*'- and *meta*-*meta*'-dimetalations using a sodium magnesiate reagent [Na<sub>4</sub>Mg<sub>2</sub>(TMP)<sub>6</sub>(<sup>*n*</sup>Bu)<sub>2</sub>] **1** (TMP is 2,2,6,6-tetramethylpiperidide) as an alkyl base (29). It functions in a templated manner, allowing double metalations to occur, and has been shown to exhibit regioselective 2,5-double alkyl basicity toward a range of substituted arenes, including amides and carbamates and

3,5-double basicity toward anilines, culminating in the isolation of a group of heterometallic inverse crown molecules (30). Here, we use the template metalation strategy to functionalize unactivated multiaryl compounds (non-DoM substrates) that lack acidity due to the absence of functional groups, regioselectively at *meta* sites. The biphenyl motif (Fig. 1A) is an important building block in the pharmaceutical, agrochemical, and polymer/materials sciences. It is present in telmisartan, valsartan, and oritavancin and is a key component of molecules for organic light-emitting devices, such as *N,N'*-di(1-naphthyl)-*N,N'*-diphenyl-(1,1'-biphenyl)-4,4'-diamine (NPB) and 4,4'-bis(*N*-carbazolyl)-1,1'-biphenyl (CPB). Biphenyl-based hydrocarbons, such as terphenyls and 1,3,5-triphenylbenzene (tpb) (Fig. 1B), are also cores for molecules used in the devices and for the synthesis of nanomaterials, such as graphene/graphene nanoribbons (31). Novel methods to improve the preparation of functionalized multiarenes for these applications are continuously being sought. Reflecting the importance of developing new methods to access novel polyaryl systems, Suzuki *et al.* (32) have recently reported the elegant synthesis of a new class of “multitalented” hexaarylbenzenes (33) that contain five or six different arene substituents on a single benzene molecule.

## RESULTS AND DISCUSSION

We targeted the templated metalation of simple polyaryl compounds (namely, biphenyl, *para*-terphenyl, *meta*-terphenyl, tpb, and antiaromatic biphenylene) using **1** and subsequently transformed the organometallic intermediates into new versatile organic precursors (34). Because of their lack of DGs (hence, the absence of docking site and strong acidifying group), the substrates studied are difficult to metalate using conventional *s*-block organometallics, unless a Lewis basic functionality activates them. Inkings that this work may be successful stemmed from the fact that we had previously shown that **1** can be used to doubly metalate naphthalene at the 1 and 4 positions regioselectively, which can be subsequently converted to 1,4-diiodonaphthalene (35).

Substituted biphenyls are often prepared by coupling reactions (36). In terms of metalation chemistry, both rings of biphenyl can be singly deprotonated using two equivalents of *n*-butyllithium/TMEDA (*N,N,N',N'*-tetramethylethylenediamine) (37). Synthetically useful yields of monolithiobiphenyls can be obtained using lithium-halogen exchange reactions (38, 39). Introducing a wholly new situation,

<sup>1</sup>WestCHEM, Department of Pure and Applied Chemistry, University of Strathclyde, 295 Cathedral Street, Glasgow G1 1XL, UK. <sup>2</sup>Strathclyde Institute of Pharmacy and Biomedical Sciences, University of Strathclyde, 161 Cathedral Street, Glasgow G4 0RE, UK.

\*Present address: Department of Chemistry, University of Oxford, Oxford OX1 3PA, UK. †Corresponding author. Email: charlie.ohara@strath.ac.uk

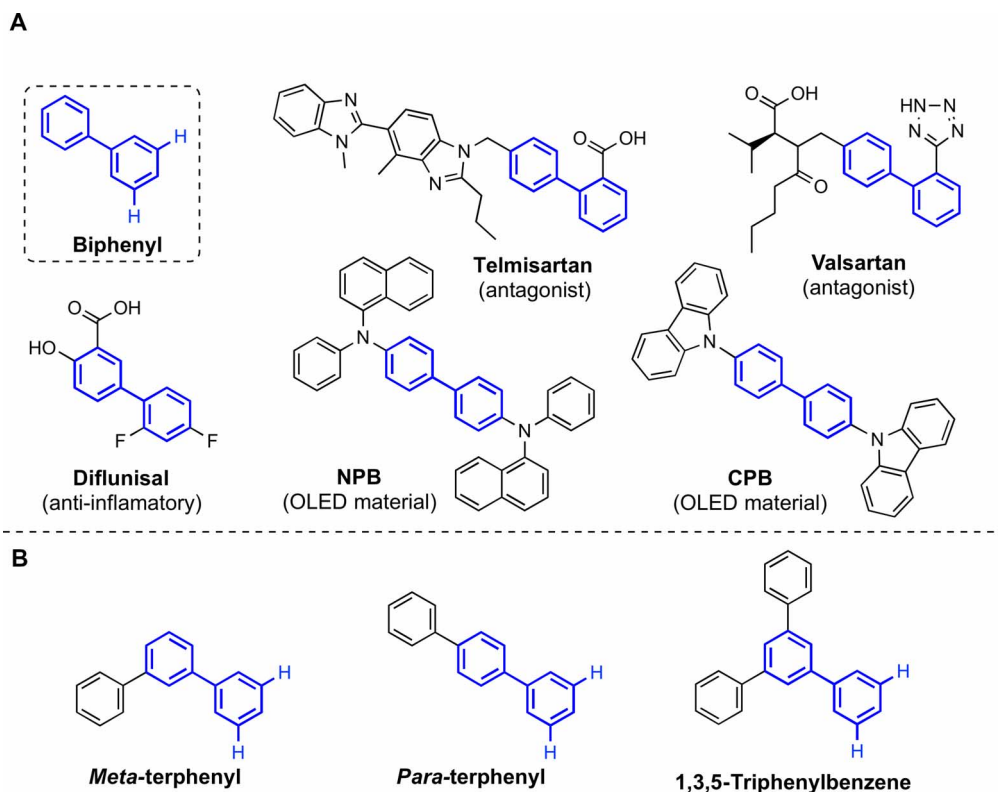


**Fig. 1. Prevalence of the biphenyl skeleton in pharmaceutical compounds and organic light-emitting diode materials. (A)** Biphenyl and the structural prevalence of its framework in pharmaceutical agents and host materials for organic light-emitting diodes (OLED). **(B)** Biphenyl-based polyaryl hydrocarbons.

by treating biphenyl with a methylcyclohexane solution of **1** in a 1:1 molar ratio, it is possible to regioselectively dimagnesiate biphenyl at the 3 and 5 positions of a single phenyl ring, as evidenced by nuclear magnetic resonance (NMR) spectroscopic analysis of the reaction mixture.  $[\text{Na}_4\text{Mg}_2(\text{TMP})_6(3,5\text{-biphenyl-di-ide})]$  **2** was isolated in 70% yield and characterized by x-ray crystallography (Fig. 2A). When two or more equivalents of **1** were used, **2** was again observed, presumably because of the high steric protection afforded to the second phenyl ring, disfavoring further reactivity. When biphenyl is treated with one or two equivalents of the monometallic reagents NaTMP or  $\text{TMPMg}^t\text{Bu}$ , intact unreacted biphenyl was obtained (Supplementary Materials). The key bond parameters of **2** (Supplementary Materials) resemble those of other comparable inverse crown molecules (29, 40). When **2** is reacted with an excess of iodine/tetrahydrofuran (THF) solution, 3,5-diiodobiphenyl **3** can be prepared in 64% isolated yield (Fig. 3, i).

The next arene molecules studied were *meta*- and *para*-terphenyl. Terphenylide anions—prepared via lithium-halogen exchange reactions of 1-halo-2,5-diphenylbenzenes and *n*-butyllithium—are useful ligands in coordination chemistry because they provide a pocket, which protects the metal from forming oligomers despite occupying only one coordination site. Power exploited this special chemistry using a bulky *meta*-terphenyl, 2,6-bis-[(2,6-diisopropyl)phenyl]phenyl to isolate the first quintuple bond between two metals, namely, two Cr(I) cations (41). It appears that the parent terphenyls have not thus far been deprotonated using any base. Focusing on *para*-terphenyl, when treated with an equivalent of **1** in methylcyclohexane solution, NMR spectroscopic analysis showed dimetalation of the arene at 3,5 positions of a single phenyl ring, likely producing  $[\text{Na}_4\text{Mg}_2(\text{TMP})_6(3,5\text{-para-terphenyl-di-ide})]$  **4**

(Supplementary Materials). Because of its high solubility, **4** was isolated in low to moderate yield (26%). An in situ mixture was reacted with iodine/THF solution and successfully converted to 3,5-diiodo-*para*-terphenyl **5** in 59% yield (Fig. 3, ii). As well as characterization by NMR spectroscopy, good quality crystals of **5** were successfully grown from an ethanol solution and were characterized by x-ray crystallography (Supplementary Materials). Increasing the base/substrate ratio (to 2:1) allowed further metalation of the *para*-terphenyl ligand to occur presumably because of the greater distance between the two “outer” phenyl rings (when compared with biphenyl), as evidenced by NMR spectroscopy. Crystals were obtained, which after x-ray analysis showed fourfold metalation of *para*-terphenyl culminating in the isolation of  $\{[\text{Na}_4\text{Mg}_2(\text{TMP})_6]_2(3,3'',5,5''\text{-para-terphenyl-tetra-ide})\}$  **6** in 69% yield (Fig. 2B). The outer rings of the *para*-terphenyl have each been doubly metalated, and each affected “arene dianion” is hosted by separate inverse crown rings. The key metrics of the inverse crown rings in **6** are essentially identical to those in the biphenyl derivative **2**. Complex **6** represents the first example of a molecule, which contains two inverse crowns within its molecular structure. Previously, it has been shown that metallocenes can also be tetradeprotonated; however, these tetranions are accommodated within a single 16-membered inverse crown ring (42, 43). When isolated **6** is reacted with iodine/THF, NMR spectroscopy reveals that it is transformed to 3,3'',5,5''-tetraiodo-*para*-terphenyl **7** in 51% yield (Fig. 3, ii). When an in situ mixture of **6** is reacted with excess iodine/THF to prepare **7**, a slightly lower yield (44%) was obtained.

The chemistry observed with *meta*-terphenyl (to produce **8** to **11**) essentially mirrors that of **4** to **7**, that is, di- and tetrametalated

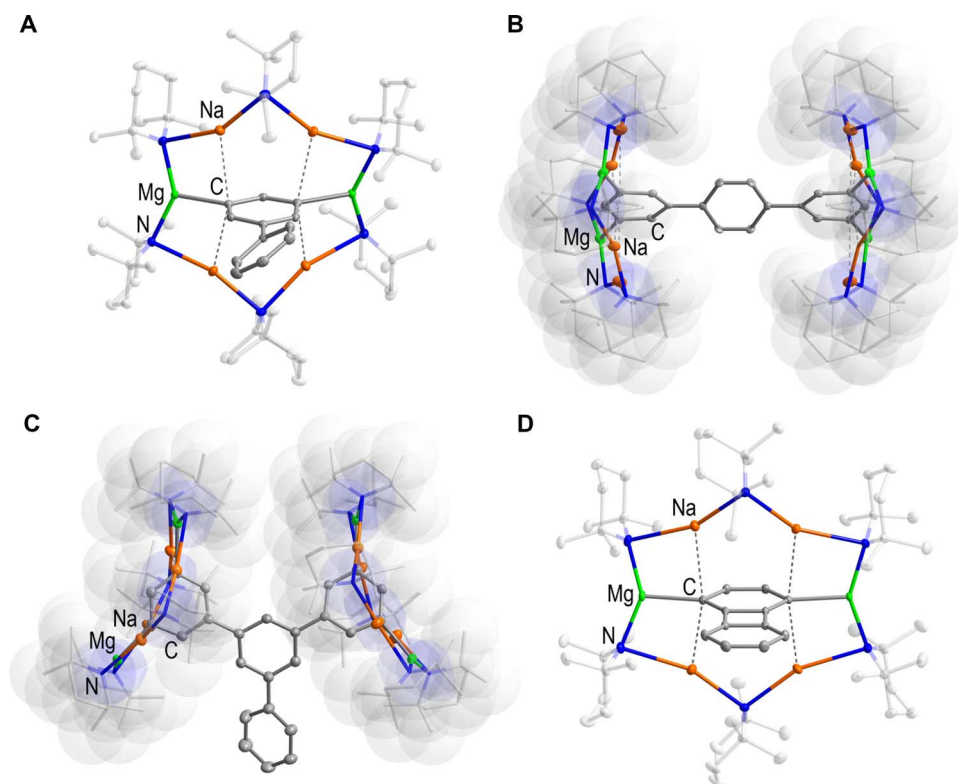


**Fig. 2. Molecular structures of isolated intermediates.** (A) **2**. (B) **6**. (C) **12**. (D) **14**. Hydrogen atoms, methylcyclohexane solvent molecules of crystallization, and disordered components of TMP and arene moieties are omitted for clarity. Displacement ellipsoids are displayed at 35% probability with the TMP frameworks pictures as capped sticks with translucent space-filling van der Waals surfaces for a probe of 1.5 Å radius for **6** and **12**.

compounds  $\{[\text{Na}_4\text{Mg}_2(\text{TMP})_6]_2(3,5\text{-}i\text{-meta-terphenyl-di-ide})\}$  **8** and  $\{[\text{Na}_4\text{Mg}_2(\text{TMP})_6]_2(3,3'',5,5''\text{-}i\text{-meta-terphenyl-tetra-ide})\}$  **10**, respectively, were obtained and characterized by NMR spectroscopy, as well as their respective di- and tetraiodo derivatives 3,5-diiodo-*meta*-terphenyl **9** (54%) and 3,3'',5,5''-tetraiodo-*meta*-terphenyl **11** (40%).

Turning to tpb, it has emerged in recent years as an important ligand, formally allowing stabilization of Ca(I) cations (44). C–H metalation of tpb is rare, and complexes derived from it generally emerge from the use of a pre-halo-substituted (normally at the central C<sub>6</sub> ring) reagent. One example of where a genuine C–H metalation is observed is when 1-bromo-2,4,6-triphenylbenzene is reacted with 2 molar equivalents of *n*-butyllithium (45). The first equivalent of alkyl-lithium induces a metal-bromine exchange, and the second metalates an interannular *peri*-C–H bond, formally giving rise to a dianion of triphenylbenzene (46). Structurally, tpb seemed an intriguing reagent to metalate. If the reaction was in keeping with the aforementioned results, it could be envisaged that di-, tetra-, or perhaps hexadeprotonation would be possible. In reality, when the arene is reacted with 1 to 3 molar equivalents of **1**, the sole isolated product is the tetradeprotonated variant  $\{[\text{Na}_4\text{Mg}_2(\text{TMP})_6]_2\{3,3'',5,5''\text{-}(1',3',5'\text{-triphenylbenzene})\text{-tetra-ide}\}$  **12** (Fig. 2C). A twofold deprotonation of tpb was not detected, perhaps because of the more acidic nature of tpb (in comparison with *meta*-terphenyl) due to the presence of the third phenyl group withdrawing electron density from the other two phenyl rings. When **6** is compared with **12**, there is a marked difference in the positions and orientations of the inverse crown rings (Fig. 2B versus Fig. 2C). In **6**, they adopt a mutual convex orientation residing in a position toward the periphery of the metalated phenyl rings. Likely because of the extra steric

demand of the additional phenyl group in tpb, the inverse crowns adopt a mutual concave orientation in **12**, residing in a position more toward the center of the metalated rings. These pronounced structural differences highlight the conformational flexibility of the template, allowing spatially distinct arenes to be accommodated. By reacting **12** with an excess of iodine/THF, it can be smoothly transformed to its tetraiodo relative 3,3'',5,5''-tetraiodo-1',3',5'-triphenylbenzene **13** in 61% yield.

Finally, we turned our attention to the prototypical antiaromatic compound biphenylene. Again, reports detailing the direct metalation of biphenylene are very scarce. When reacted with *n*- or *t*-butyllithium and quenched with electrophiles, the major species observed are the 1-substituted biphenylenes (47). When biphenylene is reacted with a methylcyclohexane solution of **1**, it was doubly metalated; however, metalation occurred simultaneously at the 1 and 4 positions to yield  $\{[\text{Na}_4\text{Mg}_2(\text{TMP})_6]_2(1,4\text{-biphenylene-di-ide})\}$  **14** (Fig. 2D). This metalation pattern is identical to that obtained with naphthalene, presumably because of the similar fused-ring nature of the substrates (thus, each arene ring is initially disubstituted) (35). Complex **14** can be converted to 1,4-diiodobiphenylene **15** in high yield (72%) by reaction with iodine/THF.

Organometallic species **2**, **4**, **6**, **8**, **10**, **12**, and **14** are soluble in  $[\text{D}_{12}]$ cyclohexane, allowing multinuclear NMR spectroscopy to be performed. A key finding is that the solid-state structures appear to be maintained in  $[\text{D}_{12}]$ cyclohexane solution (Supplementary Materials). Iodinated organic molecules **3**, **5**, **7**, **9**, **11**, **13**, and **15** are structurally simple; however, surprisingly, this study appears to represent their first synthetic routes, isolation, and full characterization. Access to these molecules has perhaps been hindered because most of polyaryl

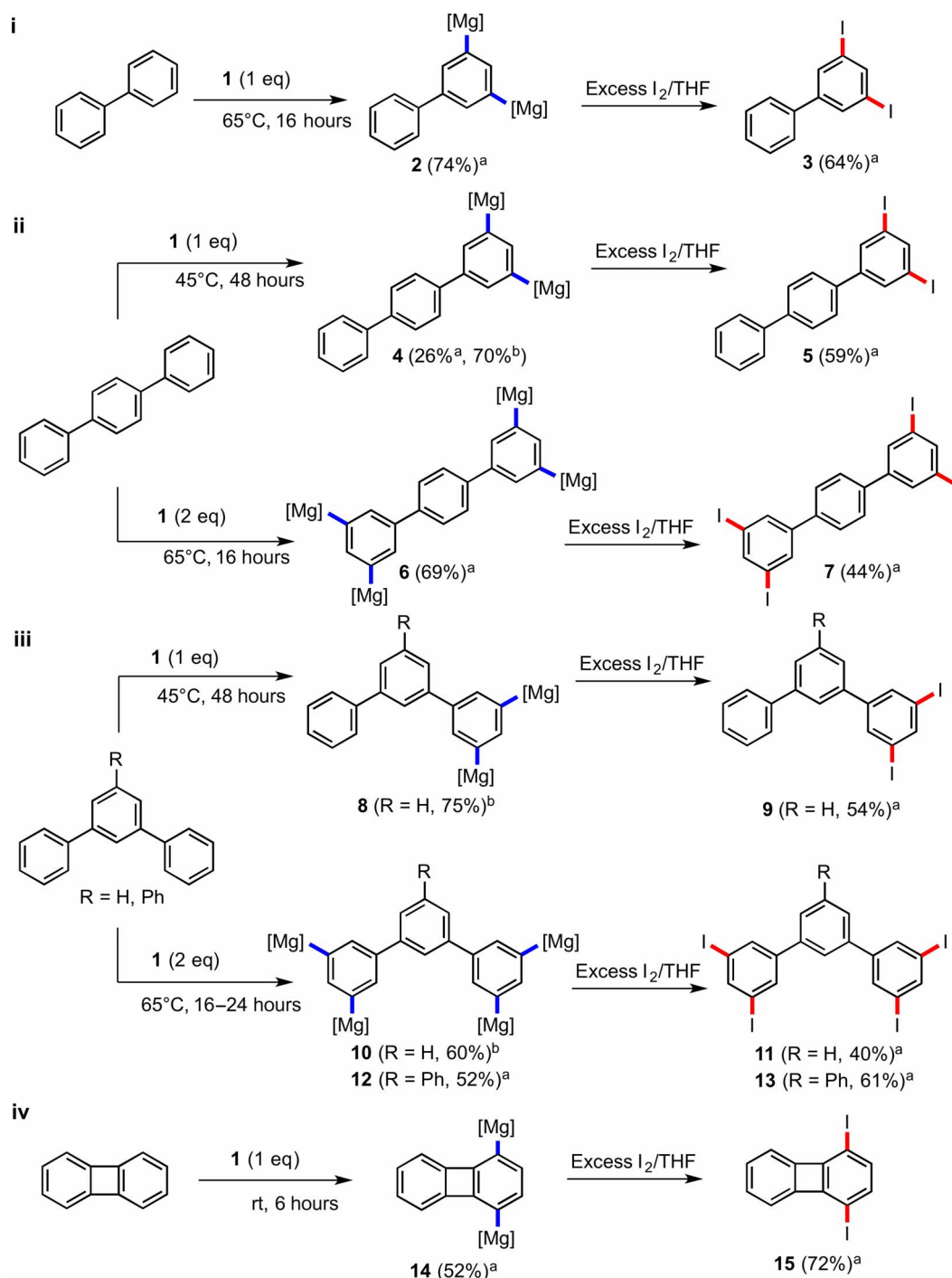


**Fig. 3. Synthetic studies for the preparation of multi-iodo polyaryl and antiaromatic compounds.** <sup>a</sup>Isolated yield. <sup>b</sup>Extent of dimetalation determined by NMR spectroscopic studies based on in situ reaction of **1** with the corresponding polyaryl substrate. [Mg] equates to  $[\text{Na}_2\text{MgTMP}_3]$ . rt, room temperature.

species are prepared via coupling reactions [for example, Suzuki-Miyaura cross-coupling (34)], so the C–I bonds in the potential synthons are themselves susceptible to coupling chemistry, thus it is difficult to prevent undesired overcoupling from occurring. The methodology presented avoids transition metal coupling chemistry, thus the iodine atoms remain intact on the arene rings, allowing further exploitation. Given the importance of iodoarenes as coupling partners in C–C

and C–heteroatom bond formation chemistry (48, 49) it is likely that these organic molecules will act as vital building blocks for the synthesis of a whole host of new functional materials. As proof of concept and illustrating the synthetic applicability of our approach, we have prepared a novel isomer of the aforementioned material CPB by converting biphenyl to 3,5-bis(*N*-carbazolyl)-1,1'-biphenyl **16** in high yield (81%; Fig. 4) via copper-catalyzed Ullmann-type coupling of carbazole with **3**.

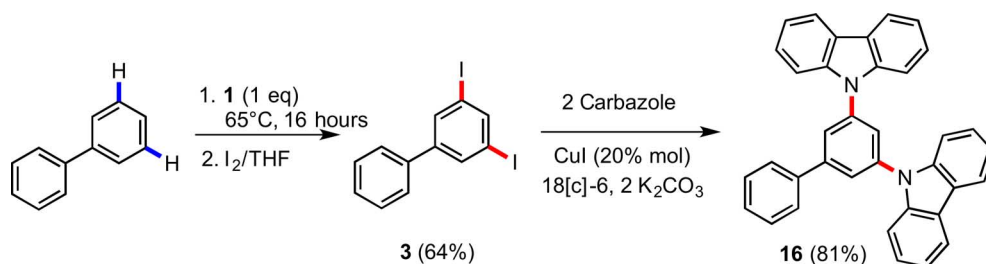


Fig. 4. Utilization of 1,3-diiodobiphenyl for Ullmann coupling reaction with carbazole for the preparation of 16.

## MATERIALS AND METHODS

### General methods and chemicals

All reactions and manipulations were performed under a protective atmosphere of dry pure argon gas using standard Schlenk techniques unless otherwise stated. *n*-Hexane was dried by heating it to reflux over sodium benzophenone ketyl and used freshly distilled under nitrogen atmosphere. Methylcyclohexane was distilled over sodium metal under nitrogen and then stored with activated 4 Å molecular sieves under argon before use. Anhydrous *N,N'*-dimethylformamide (DMF) was purchased from Sigma-Aldrich and used without further purification. [ $D_{12}$ ]cyclohexane and [ $D_6$ ]benzene were degassed and stored over activated 4 Å molecular sieves under argon before use. 2,2,6,6-Tetramethylpiperidine [TMP(H)] was purchased from Merck KGaA and stored over activated molecular sieves (4 Å).  $^{n}\text{BuLi}$  (1.6 M in hexanes) and  $^{n}\text{Bu}_2\text{Mg}$  (1 M in heptane) solutions were purchased from Sigma-Aldrich and titrated before use. Copper iodide, carbazole, potassium carbonate, 18-crown-6, sodium thiosulfate, iodine, anhydrous magnesium sulfate, ammonium chloride, and sodium chloride were purchased from Sigma-Aldrich and used as received.  $^{n}\text{BuNa}$  (50), NaTMP (51), and TMPMg  $^{n}\text{Bu}$  (29, 52) were prepared according to literature methods and used as solids from a glove box or in situ. Sodium *tert*-butoxide was purchased from Sigma-Aldrich and dried under vacuum at 150°C in a Schlenk tube for 30 min before use. Biphenyl, *meta*-terphenyl (1,3-diphenylbenzene), *para*-terphenyl (1,4-diphenylbenzene), and tpb were purchased from Sigma-Aldrich and used without further purification. Biphenylene was prepared according to the reported method and used as a crystalline solid (37).  $^{n}\text{BuNa}$ , NaTMP, TMPMg  $^{n}\text{Bu}$ , and the organometallic products 2, 4, 6, 12, and 14 were isolated and handled inside an argon-filled glove box, whereas the derivatives 8 and 10 were in situ prepared and used as methylcyclohexane solutions. Organic products 3, 5, 7, 9, 11, 13, 15, and 16 were isolated without the need of protocols to exclude atmospheric oxygen or moisture. NMR spectra were recorded on a Bruker DPX 400 MHz spectrometer, operating at 400.1 and 100.6 MHz for  $^1\text{H}$  and  $^{13}\text{C}$  NMR, respectively. The NMR assignments were performed using  $^{13}\text{C}\{^1\text{H}\}$ -DEPT135,  $^1\text{H}$ ,  $^1\text{H}$ -COSY,  $^1\text{H}$ ,  $^{13}\text{C}$ -HSQC, and  $^1\text{H}$ ,  $^{13}\text{C}$ -HMBC experiments.  $^1\text{H}$  and  $^{13}\text{C}\{^1\text{H}\}$  chemical shifts were expressed in parts per million ( $\delta = \text{ppm}$ ) and referenced to residual solvent peaks. All coupling constants ( $J$ ) are absolute values (hertz), and the description of signals are br for broad, s for singlet, d for doublet, dd for doublet of doublets, t for triplet, tt for triplet of triplets, q for quartet, and m for multiplet. Elemental analyses (triplicate) were carried out using a PerkinElmer 2400 elemental analyzer. Low-resolution mass spectra for products 3, 5, 7, 9, 11, 13, 15, and 16 were recorded on either an Agilent 7890A instrument coupled to an Agilent 5975C mass spectrometer (gas chromatography–mass spectrometry, either chemical or electron ionization mode) with helium as a carrier gas at 1 ml/min and using an Restek Rxi-5Sil-MS column (30 m  $\times$  250  $\mu\text{m}$   $\times$  0.25  $\mu\text{m}$ )

or an Kratos-Shimadzu Axima CFR MALDI-TOF spectrometer (no matrix) in positive ion mode. Accurate mass spectra were obtained at the University of Swansea in the Engineering and Physical Science Research Council (EPSRC) National Mass Spectrometry Facility, and spectra were recorded using either a Waters GCT Premier benchtop orthogonal acceleration time-of-flight mass spectrometer (electron impact ionization mode) or a Waters Xevo G2-S using the atmospheric solids analysis probe in positive mode. Values are reported as mass/charge ratio ( $m/z$ ).

### Preparation of metalating reagent 1

Solutions of 1 (0.05 and 0.066 M in methylcyclohexane) were prepared in situ according to literature methods (29, 35). Detailed procedures are given for the preparation of 2 to 17 in the Supplementary Materials.

### General synthesis of organometallic reagents 2, 4, 6, 8, 10, 12, and 14

In an argon-filled Schlenk tube, freshly prepared  $^{n}\text{BuNa}$  (640 mg, 8 mmol) was suspended in methylcyclohexane (24 ml), and TMP(H) (2.04 ml, 12 mmol) was then added via syringe to give NaTMP as a pale yellow suspension, which was stirred for 30 min at ambient temperature. Commercial  $^{n}\text{Bu}_2\text{Mg}$  (4 ml, 1 M solution in *n*-heptane, 4 mmol) was then added via syringe to give a 0.066 M pale yellow solution of 1 in methylcyclohexane. The metalating reagent 1 was stirred for 30 min at ambient temperature before use. Then, the appropriate polyarene was added, and the resulting reaction mixture was heated at the appropriate temperature. Where possible, crystals suitable for x-ray diffraction were grown (see full details in the Supplementary Materials). The NMR spectra of isolated amorphous solids/crystals in [ $D_{12}$ ]cyclohexane solution were obtained.

### General synthesis of organic compounds 3, 5, 7, 9, 11, 13, and 15

The corresponding organic substrate (biphenyl, *para*-terphenyl, *meta*-terphenyl, tpb, and biphenylene; 1 mmol each) was treated with an in situ solution of 1 in methylcyclohexane prepared according to the synthetic organometallic protocols described in the Supplementary Materials for 2, 4, 6, 8, 10, 12, and 14. The 0.05 M solutions of 1 in methylcyclohexane (20 ml) were used for the in situ preparation of 2, 4, 8, and 14, whereas the 0.066 M solutions of 1 in methylcyclohexane (30 ml) were used for the in situ preparation of 6, 10, and 12. All reactions were stirred at different temperatures and for different times and in situ monitored by NMR spectroscopy in either [ $D_{12}$ ]cyclohexane or [ $D_6$ ]benzene until magnesiation of the corresponding aromatic substrate was achieved to give the corresponding organometallic derivatives (table S1). After the in situ metalation step was achieved, the reaction mixture was cooled to  $-78^\circ\text{C}$  in a dry ice/acetone bath for 30 min and then added (either via cannula or disposable air-tight syringe) to an iodine solution in THF at

the same temperature. For the preparation of **3**, **5**, **9**, and **15**, 10 ml of a 1 M solution of iodine in THF was used, whereas for **7**, **11**, and **13**, 20 ml of a 1 M solution of iodine in THF was used. The resulting reaction mixtures were stirred at  $-78^{\circ}\text{C}$  for at least 3 hours and then allowed to slowly warm up to ambient temperature for a period of 24 hours. Saturated aqueous  $\text{NH}_4\text{Cl}$  solution ( $\sim 10$  ml) was then added, followed by saturated aqueous  $\text{Na}_2\text{S}_2\text{O}_3$  solution ( $\sim 10$  ml) until bleaching occurred. The crude mixture was extracted with EtOAc ( $3 \times 20$  ml), and the combined organic layers were washed with brine (20 ml) and dried over anhydrous  $\text{MgSO}_4$ . The solvent was removed in a rotary evaporator, and the crude product was purified by flash column chromatography (silica gel and *n*-hexane/ethyl acetate) to yield the pure title compound. Alternatively, **7** can be prepared in 51% yield by reacting **6** (1 mmol) with an iodine/THF solution (20 mmol iodine/20 ml THF). The organic derivatives **3**, **5**, **7**, **13**, and **15** can be crystallized from either MeOH, EtOH, or EtOAc. Compounds **7**, **11**, and **13** exhibit low solubility in commonly used organic solvents, which hinders their isolation and purification in the scale used in their preparations.

### Synthesis of 16

In an argon-filled Schlenk tube, 3,5-diiodo-1,1'-biphenyl (150 mg, 0.37 mmol) was mixed with carbazole (140 mg, 0.83 mmol), potassium carbonate (114 mg, 0.83 mmol), copper(I) iodide (32 mg, 0.17 mmol), and 18-crown-6 (30 mg, 0.1 mmol). Then, anhydrous DMF was added (5 ml), and the reaction mixture was refluxed for 24 hours under argon atmosphere. After cooling down to ambient temperature, the reaction mixture was filtered through a short pad of Celite, and the solvent was removed under vacuum. The crude product was purified by flash column chromatography (silica gel and *n*-hexane/ethyl acetate) to form **16** as a pale yellow solid (0.145 g, 81%). Compound **16** can be crystallized from ethyl acetate by slow evaporation to give colorless block-like crystals suitable for an x-ray diffraction study (see the Supplementary Materials for NMR spectroscopic and mass spectral data).

### SUPPLEMENTARY MATERIALS

Supplementary material for this article is available at <http://advances.sciencemag.org/cgi/content/full/3/6/e1700832/DC1>

Detailed experimental procedures

Materials and methods

Synthetic procedures

X-ray crystallography

Supplementary text

NMR spectra

fig. S1. Sections of the  $^1\text{H}$  NMR (400.1 MHz;  $[\text{D}_2]_2$ cyclohexane, 300 K) spectra showing the nonaromatic resonances for biphenylene (top; black), reaction mixture containing two conformers of **14** (middle; blue), and isolated  $[\text{Na}_4\text{Mg}_2(\text{TMP})_6(1,4\text{-biphenylene-di-ide})] \textbf{14}$  (bottom; major conformer).

fig. S2.  $^1\text{H}$ ,  $^1\text{H}$ -COSY NMR (400.1 MHz;  $[\text{D}_2]_2$ cyclohexane, 300 K) spectrum showing the nonaromatic resonances for the two conformers of **14**.

fig. S3. Sections of experimental and simulated  $^1\text{H}$  NMR spectra of **14**.

fig. S4. Sections of experimental and simulated  $^1\text{H}$  NMR spectra of **15**.

fig. S5. Molecular structure of **2** showing the contents of the asymmetric unit cell.

fig. S6. Molecular structure of **3** and its extended packing.

fig. S7. Molecular structure of **5** and its extended packing.

fig. S8. Molecular structure of **6** showing atomic connectivity.

fig. S9. Molecular structure of **12** showing the contents of the asymmetric unit cell.

fig. S10. Molecular structure of **13** and its extended packing.

fig. S11. Molecular structure of **14** showing the contents of the asymmetric unit cell.

fig. S12. Molecular structure of **15** and its extended packing.

fig. S13. Molecular structure of **16** showing the contents of the asymmetric unit cell.

fig. S14.  $^1\text{H}$  NMR study (400.1 MHz;  $[\text{D}_2]_2$ cyclohexane, 300 K) of biphenyl (top; red) and a control reaction of biphenyl and NaTMP in a 1:2 M ratio in methylcyclohexane after 24 hours at  $65^{\circ}\text{C}$  (bottom; blue).

fig. S15.  $^1\text{H}$  NMR study (400.1 MHz;  $[\text{D}_2]_2$ cyclohexane, 300 K) of biphenyl (top; red) and a control reaction of biphenyl and  $^n\text{BuMgTMP}$  in a 1:2 M ratio in methylcyclohexane after 16 hours at  $65^{\circ}\text{C}$  (bottom; blue).

fig. S16. Representative example of 3,5-dimetallation of biphenyl to give **2**.

fig. S17.  $^1\text{H}$  NMR (400.1 MHz;  $[\text{D}_2]_2$ cyclohexane, 300 K) spectrum of **2**.

fig. S18.  $^{13}\text{C}\{^1\text{H}\}$  NMR (100.6 MHz;  $[\text{D}_2]_2$ cyclohexane, 300 K) spectrum of **2**.

fig. S19. Sections of the  $^1\text{H}$ ,  $^1\text{H}$ -COSY NMR (400.1 MHz;  $[\text{D}_2]_2$ cyclohexane, 300 K) spectrum of **2**.

fig. S20. Sections of the phase-sensitive  $^1\text{H}$ ,  $^{13}\text{C}$ -HSQC NMR (400.1 MHz;  $[\text{D}_2]_2$ cyclohexane, 300 K) spectrum of **2**.

fig. S21. Sections of the  $^1\text{H}$ ,  $^{13}\text{C}$ -HMBC NMR (400.1 MHz;  $[\text{D}_2]_2$ cyclohexane, 300 K) spectrum of **2**.

fig. S22. Sections of the  $^1\text{H}$  NMR (400.1 MHz;  $[\text{D}_2]_2$ cyclohexane, 300 K) spectra of biphenyl (top; red) and **2** (bottom; blue) showing the aromatic resonances.

fig. S23. Sections of the  $^{13}\text{C}\{^1\text{H}\}$  NMR (100.6 MHz;  $[\text{D}_2]_2$ cyclohexane, 300 K) spectra of biphenyl (top; red) and **2** (bottom; blue) showing the aromatic resonances.

fig. S24.  $^1\text{H}$  NMR (400.1 MHz;  $\text{CDCl}_3$ , 300 K) spectrum of **3**.

fig. S25.  $^{13}\text{C}\{^1\text{H}\}$  NMR (100.6 MHz;  $\text{CDCl}_3$ , 300 K) spectrum of **3**.

fig. S26.  $^1\text{H}$ ,  $^1\text{H}$ -COSY NMR (400.1 MHz;  $\text{CDCl}_3$ , 300 K) spectrum of **3**.

fig. S27.  $^1\text{H}$ ,  $^{13}\text{C}$ -HSQC NMR (400.1 MHz;  $\text{CDCl}_3$ , 300 K) spectrum of **3**.

fig. S28.  $^1\text{H}$ ,  $^{13}\text{C}$ -HMBC NMR (400.1 MHz;  $\text{CDCl}_3$ , 300 K) spectrum of **3**.

fig. S29.  $^1\text{H}$  NMR (400.1 MHz;  $[\text{D}_2]_2$ cyclohexane, 300 K) spectrum of an in situ sample of **4**.

fig. S30.  $^1\text{H}$  NMR (400.1 MHz;  $\text{CDCl}_3$ , 300 K) spectrum of **5**.

fig. S31.  $^{13}\text{C}\{^1\text{H}\}$  NMR (100.6 MHz;  $\text{CDCl}_3$ , 300 K) spectrum of **5**.

fig. S32.  $^1\text{H}$ ,  $^1\text{H}$ -COSY NMR (400.1 MHz;  $\text{CDCl}_3$ , 300 K) spectrum of **5**.

fig. S33.  $^1\text{H}$ ,  $^{13}\text{C}$ -HSQC NMR (400.1 MHz;  $\text{CDCl}_3$ , 300 K) spectrum of **5**.

fig. S34. Sections of the  $^1\text{H}$ ,  $^{13}\text{C}$ -HMBC NMR (400.1 MHz;  $\text{CDCl}_3$ , 300 K) spectrum of **5**.

fig. S35.  $^1\text{H}$  NMR (400.1 MHz;  $[\text{D}_2]_2$ cyclohexane/ $\text{C}_7\text{H}_{14}$ , 300 K) spectrum of  $[\text{Na}_8\text{Mg}_4(\text{TMP})_{12}(3,3',5,5'\text{-para-terphenyl-tetra-ide})] \textbf{6}$ .

fig. S36. Section of the  $^1\text{H}$ ,  $^1\text{H}$ -COSY NMR (400.1 MHz;  $[\text{D}_2]_2$ cyclohexane/ $\text{C}_7\text{H}_{14}$ , 300 K) spectrum of  $[\text{Na}_8\text{Mg}_4(\text{TMP})_{12}(3,3',5,5'\text{-para-terphenyl-tetra-ide})] \textbf{6}$  showing the cross peaks for the aromatic resonances.

fig. S37. Sections of the  $^1\text{H}$  NMR (400.1 MHz;  $[\text{D}_2]_2$ cyclohexane, 300 K) spectra of *para*-terphenyl (top; green), **4** (middle; red), and  $[\text{Na}_8\text{Mg}_4(\text{TMP})_{12}(3,3',5,5'\text{-para-terphenyl-tetra-ide})] \textbf{6}$  (bottom; blue).

fig. S38.  $^1\text{H}$  NMR (400.1 MHz;  $\text{CDCl}_3$ , 300 K) spectrum of **7**.

fig. S39.  $^{13}\text{C}$  NMR (100.6 MHz;  $\text{CDCl}_3$ , 300 K) spectrum of **7**.

fig. S40.  $^1\text{H}$  NMR (400.1 MHz;  $[\text{D}_2]_2$ cyclohexane, 300 K) spectrum of  $[\text{Na}_4\text{Mg}_2(\text{TMP})_6(3,5\text{-meta-terphenyl-di-ide})] \textbf{8}$ .

fig. S41.  $^{13}\text{C}\{^1\text{H}\}$  NMR (100.6 MHz;  $[\text{D}_2]_2$ cyclohexane, 300 K) spectrum of  $[\text{Na}_4\text{Mg}_2(\text{TMP})_6(3,5\text{-meta-terphenyl-di-ide})] \textbf{8}$ .

fig. S42.  $^1\text{H}$  NMR (400.1 MHz; 300 K,  $\text{CDCl}_3$ ) spectrum of **9**.

fig. S43.  $^{13}\text{C}\{^1\text{H}\}$  NMR (100.6 MHz; 300 K,  $\text{CDCl}_3$ ) spectrum of **9**.

fig. S44.  $^1\text{H}$ ,  $^1\text{H}$ -COSY NMR (400.1 MHz; 300 K,  $\text{CDCl}_3$ ) spectrum of 3,5-diiodo-*meta*-terphenyl **9**.

fig. S45.  $^1\text{H}$ ,  $^{13}\text{C}$ -HSQC NMR (400.1 MHz; 300 K,  $\text{CDCl}_3$ ) spectrum of **9**.

fig. S46.  $^1\text{H}$ ,  $^{13}\text{C}$ -HMBC NMR (400.1 MHz; 300 K,  $\text{CDCl}_3$ ) spectrum of **9**.

fig. S47.  $^1\text{H}$  NMR (400.1 MHz;  $[\text{D}_2]_2$ cyclohexane, 300 K) spectrum of  $[\text{Na}_8\text{Mg}_4(\text{TMP})_{12}(3,3',5,3'\text{-meta-terphenyl-tetra-ide})] \textbf{10}$ .

fig. S48. Sections of the  $^1\text{H}$  NMR (400.1 MHz;  $[\text{D}_2]_2$ cyclohexane, 300 K) spectra of *meta*-terphenyl (top; green),  $[\text{Na}_4\text{Mg}_2(\text{TMP})_6(3,5\text{-meta-terphenyl-di-ide})] \textbf{8}$  (middle; red), and  $[\text{Na}_8\text{Mg}_4(\text{TMP})_{12}(3,3',5,3'\text{-meta-terphenyl-tetra-ide})] \textbf{10}$  (bottom; blue) showing the aromatic resonances.

fig. S49.  $^1\text{H}$  NMR (400.1 MHz;  $\text{CDCl}_3$ , 300 K) spectrum of **11**.

fig. S50.  $^{13}\text{C}\{^1\text{H}\}$  NMR (100.6 MHz;  $\text{CDCl}_3$ , 300 K) spectrum of **11**.

fig. S51.  $^1\text{H}$ ,  $^1\text{H}$ -COSY NMR (400.1 MHz;  $\text{CDCl}_3$ , 300 K) spectrum of **9**.

fig. S52.  $^1\text{H}$ ,  $^{13}\text{C}$ -HSQC NMR (400.1 MHz;  $\text{CDCl}_3$ , 300 K) spectrum of **9**.

fig. S53.  $^1\text{H}$ ,  $^{13}\text{C}$ -HMBC NMR (400.1 MHz;  $\text{CDCl}_3$ , 300 K) spectrum of **9**.

fig. S54.  $^1\text{H}$  NMR (400.1 MHz;  $[\text{D}_6]_6$ benzene, 300 K) spectrum of  $[\text{Na}_8\text{Mg}_4(\text{TMP})_{12}(3,3',5,5'\text{-}(1',3',5'\text{-triphenylbenzene-tetra-ide})] \textbf{12}$ .

fig. S55. Section of the  $^1\text{H}$ ,  $^1\text{H}$ -COSY NMR (400.1 MHz;  $[\text{D}_6]_6$ benzene, 300 K) spectrum of **12** showing the cross peaks for the aromatic resonances.

fig. S56.  $^1\text{H}$  NMR (400.1 MHz;  $[\text{D}_6]_6$ benzene, 300 K) spectra of tpb (top; red) and **12** (bottom; blue).

fig. S57.  $^1\text{H}$  NMR (400.1 MHz;  $\text{CDCl}_3$ , 300 K) spectrum of 3,3',5,5'-tetraiodo-5'-phenyl-benzene **13**.

fig. S58.  $^{13}\text{C}\{^1\text{H}\}$  NMR (100.6 MHz;  $\text{CDCl}_3$ , 300 K) spectrum of **13**.

fig. S59.  $^1\text{H}$ ,  $^1\text{H}$ -COSY NMR (400.1 MHz;  $\text{CDCl}_3$ , 300 K) spectrum of **13**.

fig. S60.  $^1\text{H}$ ,  $^{13}\text{C}$ -HSQC NMR (400.1 MHz;  $\text{CDCl}_3$ , 300 K) spectrum of **13**.

fig. S61.  $^1\text{H}$ ,  $^{13}\text{C}$ -HMBC NMR (400.1 MHz;  $\text{CDCl}_3$ , 300 K) spectrum sections of **13**.

fig. S62.  $^1\text{H}$  NMR (400.1 MHz;  $[\text{D}_2]_2$ cyclohexane, 300 K) spectrum of **14**.

fig. S63.  $^{13}\text{C}\{^1\text{H}\}$  NMR (100.6 MHz;  $[\text{D}_2]_2$ cyclohexane, 300 K) spectrum of **14**.

fig. S64. Sections of the  $^1\text{H}$ ,  $^1\text{H}$ -COSY NMR (400.1 MHz;  $[\text{D}_2]_2$ cyclohexane, 300 K) spectrum of **14**.

fig. S65. Sections of the phase-sensitive  $^1\text{H}$ ,  $^{13}\text{C}$ -HSQC NMR (400.1 MHz;  $[\text{D}_2]_2$ cyclohexane, 300 K) spectrum of **14**.

fig. S66. Sections of the  $^1\text{H}$ ,  $^{13}\text{C}$ -HMBC NMR (400.1 MHz;  $[\text{D}_2]_2$ cyclohexane, 300 K) spectrum of **14**.

fig. S67.  $^{13}\text{C}\{^1\text{H}\}$  NMR (100.6 MHz;  $[\text{D}_2]$ cyclohexane, 300 K) section of the spectra of biphenylene (top; red) and isolated **14** (bottom; blue, major conformer).  
 fig. S68.  $^1\text{H}$  NMR (400.1 MHz;  $\text{CDCl}_3$ , 300 K) spectrum of **15**.  
 fig. S69.  $^{13}\text{C}\{^1\text{H}\}$  NMR (100.6 MHz;  $\text{CDCl}_3$ , 300 K) spectrum of **15**.  
 fig. S70.  $^1\text{H},^1\text{H}$ -COSY NMR (400.1 MHz;  $\text{CDCl}_3$ , 300 K) spectrum of **15**.  
 fig. S71.  $^1\text{H},^{13}\text{C}$ -HSQC NMR (400.1 MHz;  $\text{CDCl}_3$ , 300 K) spectrum of **15**.  
 fig. S72.  $^1\text{H},^{13}\text{C}$ -HMBC NMR (400.1 MHz;  $\text{CDCl}_3$ , 300 K) spectrum of **15**.  
 fig. S73.  $^1\text{H}$  NMR (400.1 MHz;  $\text{CDCl}_3$ , 300 K) spectra of biphenylene (top; red) and **15** (bottom; blue).  
 fig. S74.  $^{13}\text{C}\{^1\text{H}\}$  NMR (100.6 MHz;  $\text{CDCl}_3$ , 300 K) spectra of biphenylene (top; red) and **15** (bottom; blue).  
 fig. S75.  $^1\text{H}$  NMR (400.1 MHz;  $\text{CDCl}_3$ , 300 K) spectrum of **16**.  
 fig. S76.  $^{13}\text{C}\{^1\text{H}\}$  NMR (100.6 MHz;  $\text{CDCl}_3$ , 300 K) spectrum of **16**.  
 fig. S77.  $^1\text{H},^1\text{H}$ -COSY NMR (400.1 MHz;  $\text{CDCl}_3$ , 300 K) spectrum of **16**.  
 fig. S78.  $^1\text{H},^{13}\text{C}$ -HSQC NMR (400.1 MHz;  $\text{CDCl}_3$ , 300 K) spectrum of **16**.  
 fig. S79.  $^1\text{H},^{13}\text{C}$ -HMBC NMR (400.1 MHz;  $\text{CDCl}_3$ , 300 K) spectrum of **16**.  
 table S1. Metalation conditions and scope.  
 References (53–62)

## REFERENCES AND NOTES

1. *Organometallics in Synthesis: Third Manual*, M. Schlosser, Ed. (John Wiley & Sons, 2013).
2. H. Gilman, R. L. Bebb, Relative reactivities of organometallic compounds. XX. Metalation. *J. Am. Chem. Soc.* **61**, 109–112 (1939).
3. G. Wittig, U. Pockels, H. Droge, Über die Austauschbarkeit von aromatisch gebundenem Wasserstoff gegen Lithium mittels Phenyl-lithiums. *Ber. Dtsch. Chem. Ges.* **71**, 1903–1912 (1938).
4. V. Snieckus, Directed *ortho* metalation. Tertiary amide and *O*-carbamate directors in synthetic strategies for polysubstituted aromatics. *Chem. Rev.* **90**, 879–933 (1990).
5. P. Beak, V. Snieckus, Directed lithiation of aromatic tertiary amides: An evolving synthetic methodology for polysubstituted aromatics. *Acc. Chem. Res.* **15**, 306–312 (1982).
6. T. K. Macklin, V. Snieckus, in *Handbook of C-H Transformations*, G. Dyker, Ed. (Wiley-VCH, 2005), vol. 1, pp. 106–118.
7. M. C. Whisler, S. MacNeil, V. Snieckus, P. Beak, Beyond thermodynamic acidity: A perspective on the complex-induced proximity effect (CIPE) in deprotonation reactions. *Angew. Chem. Int. Ed.* **43**, 2206–2225 (2004).
8. T. K. Macklin, V. Snieckus, Directed *ortho* metalation methodology. The *N,N*-dialkyl aryl *O*-sulfamate as a new directed metalation group and cross-coupling partner for Grignard reagents. *Org. Lett.* **7**, 2519–2522 (2005).
9. C. Metallinos, S. Nerdinger, V. Snieckus, *N*-cumyl benzamide, sulfonamide, and aryl *O*-carbamate directed metalation groups. Mild hydrolytic lability for facile manipulation of directed *ortho* metalation derived aromatics. *Org. Lett.* **1**, 1183–1186 (1999).
10. P. Beak, R. A. Brown, The *ortho* lithiation of tertiary benzamides. *J. Org. Chem.* **42**, 1823–1824 (1977).
11. M. Kauch, D. Hoppe, Synthesis of halogenated phenols by directed *ortho*-lithiation and *ipso*-iododesilylation reactions of *O*-aryl *N*-isopropylcarbamates. *Synthesis* 1578–1589 (2006).
12. J. Mortier, J. Moyroud, B. Bennetau, P. A. Cain, The carboxylic acid group as an effective director of *ortho*-lithiation. *J. Org. Chem.* **59**, 4042–4044 (1994).
13. A. Krasovskiy, V. Krasovskaya, P. Knochel, Mixed Mg/Li amides of the type  $\text{R}_2\text{NMgCl}\cdot\text{LiCl}$  as highly efficient bases for the regioselective generation of functionalized aryl and heteroaryl magnesium compounds. *Angew. Chem. Int. Ed.* **45**, 2958–2961 (2006).
14. B. Haag, M. Mosrin, H. Ila, V. Malakhov, P. Knochel, Regio- and chemoselective metalation of arenes and heteroarenes using hindered metal amide bases. *Angew. Chem. Int. Ed.* **50**, 9794–9824 (2011).
15. N. Marquise, G. Bretel, F. Lassagne, F. Chevallier, T. Roisnel, V. Dorcet, Y. S. Halauko, O. A. Ivashkevich, V. E. Matulis, P. C. Gros, F. Mongin, Deprotonation using mixed lithium–zinc and lithium–copper bases and computed CH acidity of 2-substituted quinolines. *RSC Adv.* **4**, 19602–19612 (2014).
16. K. Snégaroff, S. Komagawa, M. Yonehara, F. Chevallier, P. C. Gros, M. Uchiyama, F. Mongin, Lithium cadmate-mediated deprotonative metalation of anisole: Experimental and computational study. *J. Org. Chem.* **75**, 3117–3120 (2010).
17. D. R. Armstrong, E. Crosbie, E. Hevia, R. E. Mulvey, D. L. Ramsay, S. D. Robertson, TMP (2,2,6,6-tetramethylpiperidine)-aluminate bases: Lithium-mediated aluminon or lithiation–alkylaluminum-trapping reagents? *Chem. Sci.* **5**, 3031–3045 (2014).
18. Y. Kondo, M. Shilai, M. Uchiyama, T. Sakamoto, TMP–zincate as highly chemoselective base for directed *ortho* metalation. *J. Am. Chem. Soc.* **121**, 3539–3540 (1999).
19. M. Uchiyama, Y. Matsumoto, D. Nobuto, T. Furiyama, K. Yamaguchi, K. Morokuma, Structure and reaction pathway of TMP-zincate: Amido base or alkyl base? *J. Am. Chem. Soc.* **128**, 8748–8750 (2006).
20. C. Cheng, J. F. Hartwig, Rhodium-catalyzed intermolecular C–H silylation of arenes with high steric regiocontrol. *Science* **343**, 853–857 (2014).
21. Z. Dong, J. Wang, G. Dong, Simple amine-directed *meta*-selective C–H arylation via Pd/norbornene catalysis. *J. Am. Chem. Soc.* **137**, 5887–5890 (2015).
22. M.-H. Larraufie, G. Maestri, A. Beaume, É. Derat, C. Ollivier, L. Fensterbank, C. Courillon, E. Lacôte, M. Catellani, M. Malacria, Exception to the *ortho* effect in palladium/norbornene catalysis. *Angew. Chem. Int. Ed.* **50**, 12253–12256 (2011).
23. M. Catellani, F. Frignani, A. Rangoni, A complex catalytic cycle leading to a regioselective synthesis of *o,o'*-disubstituted vinylarenes. *Angew. Chem. Int. Ed.* **36**, 119–122 (1997).
24. J. Luo, S. Preciado, I. Larrosa, Overriding *ortho*–*para* selectivity via a traceless directing group relay strategy: The *meta*-selective arylation of phenols. *J. Am. Chem. Soc.* **136**, 4109–4112 (2014).
25. D. Leow, G. Li, T.-S. Mei, J.-Q. Yu, Activation of remote *meta*-C–H bonds assisted by an end-on template. *Nature* **486**, 518–522 (2012).
26. R.-Y. Tang, G. Li, J.-Q. Yu, Conformation-induced remote *meta*-C–H activation of amines. *Nature* **507**, 215–220 (2014).
27. S. Bag, T. Patra, A. Modak, A. Deb, S. Maity, U. Dutta, A. Dey, R. Kancharla, A. Maji, A. Hazra, M. Bera, D. Maiti, Remote *para*-C–H functionalization of arenes by a D-shaped biphenyl template-based assembly. *J. Am. Chem. Soc.* **137**, 11888–11891 (2015).
28. A. Maji, B. Bhaskararao, S. Singha, R. B. Sunoj, D. Maiti, Directing group assisted *meta*-hydroxylation by C–H activation. *Chem. Sci.* **7**, 3147–3153 (2016).
29. A. J. Martinez-Martinez, A. R. Kennedy, R. E. Mulvey, C. T. O'Hara, Strong bases. Directed *ortho*-*meta*- and *meta*-*meta*-dimetalations: A template base approach to deprotonation. *Science* **346**, 834–837 (2014).
30. R. E. Mulvey, Modern ate chemistry: Applications of synergic mixed alkali-metal–magnesium or –zinc reagents in synthesis and structure building. *Organometallics* **25**, 1060–1075 (2006).
31. K. Gharagzloo-Hubmann, N. S. Müller, M. Giersig, C. Lotze, K. J. Franke, S. Reich, Requirement on aromatic precursor for graphene formation. *J. Phys. Chem. C* **120**, 9821–9825 (2016).
32. S. Suzuki, Y. Segawa, K. Itami, J. Yamaguchi, Synthesis and characterization of hexaarylbenzenes with five or six different substituents enabled by programmed synthesis. *Nat. Chem.* **7**, 227–233 (2015).
33. V. Vij, V. Bhalla, M. Kumar, Hexaarylbenzene: Evolution of properties and applications of multitalented scaffold. *Chem. Rev.* **116**, 9565–9627 (2016).
34. J. Mortier, *Arene Chemistry: Reaction Mechanisms and Methods for Aromatic Compounds* (John Wiley & Sons Inc., 2016).
35. A. J. Martinez-Martinez, D. R. Armstrong, B. Conway, B. J. Fleming, J. Klett, A. R. Kennedy, R. E. Mulvey, S. D. Robertson, C. T. O'Hara, Pre-inverse-crowns: Synthetic, structural and reactivity studies of alkali metal magnesiate primed for inverse crown formation. *Chem. Sci.* **5**, 771–781 (2014).
36. A. Jutand, G. Lefèvre, Transition metal-catalyzed carbon–carbon cross-coupling, in *Arene Chemistry: Reaction Mechanisms and Methods for Aromatic Compounds*, J. Mortier, Ed. (John Wiley & Sons Inc., 2016), 511–545.
37. T. Schaub, U. Radius, A convenient synthesis of biphenylene. *Tetrahedron Lett.* **46**, 8195–8197 (2005).
38. Z. Liu, H. Tan, L. Wang, T. Fu, Y. Xia, Y. Zhang, J. Wang, Transition-metal-free intramolecular carbene aromatic substitution/Büchner reaction: Synthesis of fluorenes and [6,5,7]benzo-fused rings. *Angew. Chem. Int. Ed.* **54**, 3056–3060 (2015).
39. G. Bähr, R. Gelius, Organozinnverbindungen mit raumfüllenden Arylgruppen, I. *Chem. Ber.* **91**, 812–818 (1958).
40. V. L. Blair, L. M. Carrella, W. Clegg, B. Conway, R. W. Harrington, L. M. Hogg, J. Klett, R. E. Mulvey, E. Rentschler, L. Russo, Tuning the basicity of synergic bimetallic reagents: Switching the regioselectivity of the direct dimetalation of toluene from 2,5- to 3,5-positions. *Angew. Chem. Int. Ed.* **47**, 6208–6211 (2008).
41. T. Nguyen, A. D. Sutton, M. Brynda, J. C. Fettingier, G. J. Long, P. P. Power, Synthesis of a stable compound with fivefold bonding between two chromium(I) centers. *Science* **310**, 844–847 (2005).
42. W. Clegg, K. W. Henderson, A. R. Kennedy, R. E. Mulvey, C. T. O'Hara, R. B. Rowlings, D. M. Tooke, Regioselective tetrametalation of ferrocene in a single reaction: Extension of s-block inverse crown chemistry to the d-block. *Angew. Chem. Int. Ed.* **40**, 3902–3905 (2001).
43. P. Andrikopoulos, D. R. Armstrong, W. Clegg, C. J. Gilfillan, E. Hevia, A. R. Kennedy, R. E. Mulvey, C. T. O'Hara, J. A. Parkinson, D. M. Tooke, A homologous series of regioselectively tetradeprotonated group 8 metallocenes: New inverse crown ring compounds synthesized via a mixed sodium–magnesium tris(diisopropylamide) synergic base. *J. Am. Chem. Soc.* **126**, 11612–11620 (2004).
44. S. Kriek, H. Görls, L. Yu, M. Reiher, M. Westerhausen, Stable “inverse” sandwich complex with unprecedented organocalcium(I): Crystal structures of  $[(\text{thf})_2\text{Mg}(\text{Br})\text{-C}_6\text{H}_2\text{-2,4,6-Ph}_3]$  and  $[(\text{thf})_2\text{Ca}(\mu\text{-C}_6\text{H}_3\text{-1,3,5-Ph}_3)]\text{Ca}(\text{thf})_3]$ . *J. Am. Chem. Soc.* **131**, 2977–2985 (2009).
45. G. S. Girolami, M. E. Riehl, K. S. Suslick, S. R. Wilson, Rare example of a monomeric aryllithium complex. X-ray crystal structure of (2,4,6-triphenylphenyl)lithium-bis(diethyl ether). *Organometallics* **11**, 3907–3910 (1992).

46. H. A. Jenkins, D. Abeysekera, D. A. Dickie, J. A. C. Clyburne, Double lithiation of 2,4,6-triphenylbromobenzene: Synthesis of bis-amidines and an aluminium bis-amidinate complex. *J. Chem. Soc. Dalton Trans.* 3919–3922 (2002).
47. R. Beck, S. A. Johnson, Mechanistic implications of an asymmetric intermediate in catalytic C–C coupling by a dinuclear nickel complex. *Chem. Commun.* **47**, 9233–9235 (2011).
48. A. R. Lahrood, J. Björk, W. M. Heckl, M. Lackinger, 1,3-Diiodobenzene on Cu(111)—An exceptional case of on-surface Ullmann coupling. *Chem. Commun.* **51**, 13301–13304 (2015).
49. G. Zhang, M. Auer-Berger, D. W. Gehrig, P. W. M. Blom, M. Baumgarten, D. Schollmeyer, E. J. W. List-Kratochvil, K. Müllen, Blue light emitting polyphenylene dendrimers with bipolar charge transport moieties. *Molecules* **21**, E1400 (2016).
50. C. Schade, W. Bauer, P. V. R. Schleyer, n-Butylsodium: The preparation, properties and NMR spectra of a hydrocarbon- and tetrahydrofuran-soluble reagent. *J. Organomet. Chem.* **295**, C25–C28 (1985).
51. B. Gehrhus, P. H. Hitchcock, A. R. Kennedy, M. F. Lappert, R. E. Mulvey, P. J. A. Rodger, Synthesis and crystal structure of trimeric sodium 2,2,6,6-tetramethylpiperidine (NaTMP). *J. Organomet. Chem.* **587**, 88–92 (1999).
52. E. Hevia, A. R. Kennedy, R. E. Mulvey, S. Weatherstone, Synthesis and crystal structure of  $[(n\text{BuMg}(\mu\text{-TMP}))_2]$  and of a homometallic inverse crown in tetranuclear  $[(n\text{BuMg}_2[\mu\text{-N(H)Dipp}]_2[\mu_3\text{-OnBu}]_2)]$ . *Angew. Chem. Int. Ed.* **43**, 1709–1712 (2004).
53. G. M. Sheldrick, Crystal structure refinement with SHELXL. *Acta Cryst. C* **71**, 3–8 (2015).
54. C. B. Hubschle, G. M. Sheldrick, B. Dittrich, *ShelXle*: A Qt graphical user interface for SHELXL. *J. Appl. Crystallogr.* **44**, 1281–1284 (2011).
55. A. L. Spek, PLATON SQUEEZE: A tool for the calculation of the disordered solvent contribution to the calculated structure factors. *Acta Cryst. C* **71**, 9–18 (2015).
56. A. R. Katritzky, N. G. Akhmedov, A. Güven, J. Doskocz, R. G. Akhmedova, S. Majumder, C. D. Hall, gNMR simulated  $^1\text{H}$  and proton-coupled  $^{13}\text{C}$  NMR spectra of substituted 3-nitropyridines. GIAO/DFT calculated values of proton and carbon chemical shifts and coupling constants. *J. Mol. Struct.* **787**, 131–147 (2006).
57. G. Bringmann, A. J. Price Mortimer, P. A. Keller, M. J. Gresser, J. Garner, M. Breuning, Atroposelective synthesis of axially chiral biaryl compounds. *Angew. Chem. Int. Ed.* **44**, 5384–5427 (2005).
58. J. Clayden, W. J. Moran, P. J. Edwards, S. R. LaPlante, The challenge of atropisomerism in drug discovery. *Angew. Chem. Int. Ed.* **48**, 6398–6401 (2009).
59. R. Ruzziconi, S. Spizzichino, A. Mazzanti, L. Lunazzi, M. Schlosser, The biphenyl-monitored effective size of unsaturated functional or fluorinated *ortho* substituents. *Org. Biomol. Chem.* **8**, 4463–4471 (2010).
60. S. Toyota, T. Iida, C. Kunizane, N. Tanifuji, Y. Yoshida, Rotational isomerism involving an acetylenic carbon IV: Synthesis and structure of bis(1,1';3',1"-terphenyl-2'-yl)ethynes: Molecular design of sterically congested alkynes toward restricted rotation about acetylenic axis. *Org. Biomol. Chem.* **1**, 2298–2302 (2003).
61. M. Modjowski, S. V. Lindeman, R. Rathore, A versatile preparation of Geländer-type *p*-terphenyls from a readily available diacetylenic precursor. *Org. Lett.* **11**, 4656–4659 (2009).
62. L. Lunazzi, A. Mazzanti, M. Minzoni, J. E. Anderson, Structure, conformation, and dynamic processes of the stereolabile atropisomers of hindered terphenyl hydrocarbons. *Org. Lett.* **7**, 1291–1294 (2005).

#### Acknowledgments

**Funding:** We would like to thank R. Mulvey, E. Hevia, and S. Robertson for useful and insightful discussions and the financial support of the EPSRC (Career Acceleration Fellowship; EP/J001872/1 and EP/L001497/1). We are also grateful to the EPSRC UK National Mass Spectrometry Facility, Swansea, for collecting our high-resolution mass spectral data.

**Author contributions:** A.J.M.-M. carried out most of the experimental work, drafted most of the Supplementary Materials, and contributed ideas to the project. A.R.K. and I.D.H.O. ensured that the x-ray crystallography work was carried out to high level and contributed to the drafting of the manuscript. B.J.F. and S.J. carried out the initial experimental work. C.T.O. conceived and developed the project and drafted the manuscript. **Competing interests:** The authors declare that they have no competing interests. **Data and materials availability:** X-ray crystallographic data for compounds **2**, **3**, **5**, **6**, **12**, **13**, **14**, **15**, and **16** are freely available at the Cambridge Crystallographic Data Centre (CCDC 1516422–30) via [http://www.ccdc.cam.ac.uk/data\\_request/cif](http://www.ccdc.cam.ac.uk/data_request/cif). The research data associated with this paper are openly available at <http://dx.doi.org/10.15129/b1d7b580-838c-4621-ad43-fccd2579024d>. All other data needed to evaluate the conclusions in the paper are present in the paper and/or the Supplementary Materials. Additional data related to this paper may be requested from the authors.

Submitted 10 March 2017

Accepted 19 April 2017

Published 30 June 2017

10.1126/sciadv.1700832

**Citation:** A. J. Martínez-Martínez, S. Justice, B. J. Fleming, A. R. Kennedy, I. D. H. Oswald, C. T. O'Hara, Templated deprotonative metalation of polyaryl systems: Facile access to simple, previously inaccessible multi-iodoarenes. *Sci. Adv.* **3**, e1700832 (2017).

## Templated deprotonative metalation of polyaryl systems: Facile access to simple, previously inaccessible multi-iodoarenes

Antonio J. Martínez-Martínez, Stephen Justice, Ben J. Fleming, Alan R. Kennedy, Iain D. H. Oswald and Charles T. O'Hara

*Sci Adv* 3 (6), e1700832.  
DOI: 10.1126/sciadv.1700832

### ARTICLE TOOLS

<http://advances.sciencemag.org/content/3/6/e1700832>

### SUPPLEMENTARY MATERIALS

<http://advances.sciencemag.org/content/suppl/2017/06/26/3.6.e1700832.DC1>

### REFERENCES

This article cites 56 articles, 3 of which you can access for free  
<http://advances.sciencemag.org/content/3/6/e1700832#BIBL>

### PERMISSIONS

<http://www.sciencemag.org/help/reprints-and-permissions>

Use of this article is subject to the [Terms of Service](#)

---

*Science Advances* (ISSN 2375-2548) is published by the American Association for the Advancement of Science, 1200 New York Avenue NW, Washington, DC 20005. 2017 © The Authors, some rights reserved; exclusive licensee American Association for the Advancement of Science. No claim to original U.S. Government Works. The title *Science Advances* is a registered trademark of AAAS.